Structure-Dynamics Relationships of the α-relaxation in Flexible Copolyesters during Crystallization as Revealed by Real-Time Methods

A. Nogales[1], T.A. Ezquerra[1,*], J.M. García[2], F.J. Baltá-Calleja[1].

[1]Instituto de Estructura de la Materia, C.S.I.C. Serrano 119, Madrid 28006, Spain.

[2]Instituto de Ciencia y Tecnología de Polímeros, C.S.I.C., Juan de la Cierva 3, 28006 Madrid, Spain.

Keywords: Relaxation, real-time, bacterial, copolyester, synchrotron radiation.

Mailing Address:T.A. Ezquerra, Instituto de Estructura de la Materia, C.S.I.C., Serrano 119, Madrid 28006, Spain. Tf.:34 91 5619400, FAX:34 1 5642431, e-mail: emtibe@roca.csic.es

Abstract

The evolution of the α-relaxation during an isothermal crystallization process of a series of flexible copolyesters of hydroxybutyrate (HB) and hydroxyvalerate (HV), has been followed in real time by wide angle X-ray scattering and dielectric complex permittivity measurements. The change of the dielectric parameters with crystallization time can be phenomenologically described in terms of the Havriliak-Negami equation. The dielectric strength follows a sigmoidal-shaped pattern similar to that shown by the crystallinity. A reduction of the overall mobility with crystallization time of the polymeric chains in the amorphous phase has been observed. This slowing-down effect depends on the HV molar content. The influence of the chain flexibility on the crystalline induced restriction has been discussed in the light of similar studies carried out with more rigid polymers. Dielectric experiments suggest that the progressive immobilization of polymer segments as crystallization proceeds cannot be exclusively associated with the amount of crystalline material. Differences in microstructure, depending on the HV molar content, seem to be responsible for the observed behaviour. The progressive broadening and symmetrization of the α-relaxation with increasing crystallization time has been explained as due to a restriction of the large scale motions of the polymeric chains, as the material is being filled-in with crystals.

1 Introduction

The molecular motions occurring in the amorphous phase of a semicrystalline polymer present characteristic aspects which depend, in a first approximation, on the degree of crystallinity [1]. In semicrystalline polymers at temperatures higher than the glass transition temperature, T_g, the amorphous polymer chains are confined to move between the crystalline regions [1,2]. This restriction leads to a modification the α-relaxation which appears in polymeric systems at T_g. It is known that this relaxation involves motions extended to several molecular segments. The existence of crystallinity in a polymer is reflected in the dynamics of the α-relaxation, when compared with that of the pure amorphous polymer, by three effects: a) a decrease of the intensity of the relaxation , b) an increase of the relaxation time and c) a concurrent change in its shape [1,2,3,4,5].

In polymers, the frequency dependence of the complex dielectric permittivity, ϵ^*, deviates from the simple Debye behaviour characterized by a single relaxation time. A phenomenological description of ϵ^* is given by the Havriliak-Negami (HN) function of the form [6]:

$$\epsilon^*(\omega) = \epsilon_u + \frac{\Delta\epsilon}{[1 + (i\omega\tau_o)^b]^c} \tag{1}$$

In this equation $\Delta\epsilon = \epsilon_r - \epsilon_u$ is the dielectric strength, ϵ_r and ϵ_u being the

relaxed($\omega = 0$) and unrelaxed($\omega = \infty$) dielectric constant values, τ_0 the central relaxation time of the relaxation time distribution function and b and c the shape parameters which describe the symmetric and the asymmetric broadening of the relaxation time distribution function, respectively [6]. Schlosser and Schönhals have suggested that the shape parameters can be related to the molecular dynamics at the glass transition provided that the molecular mobility is controlled by inter and intramolecular interactions [7]. This model relates the b parameter to the large scale motions and the $b \cdot c$ product to the small scale motions. Experimental support of the model has been provided by dielectric spectroscopy techniques [8]. In addition, this model allows one to interpret the observed broadening and symmetrization of the α relaxation in a semirigid polymer during crystallization as due to restriction in the long scale motions of the polymeric chains as the material is filled in with crystals [4].

Until now most crystallization studies using dielectric relaxation, have been carried out on isothermally crystallized materials from the glassy state after subsequent quenching. Only a few dielectric measurements were performed in real time during crystallization [2,4,9,10]. In these studies, polymers with a relatively high T_g value like poly(ethylene terephthalate) (PET) or poly(aryl ether ketone)s (PEKK) were examined. This was partially so in order to avoid uncontrolled crystallization near room temperature. Flexible polymers,

having T_g values close or below room temperature are difficult to keep in the amorphous state long enough to perform physical measurements [11]. To verify whether molecular flexibility may qualitatively affect the observed modifications in the dynamics of the α relaxation described above for semirigid polymers is both an open question and an experimental challenge.

In the present paper we study the evolution of the dielectric behaviour of a series of amorphous flexible polymers during the crystallization process. In order to follow the changes in the α- relaxation a series of copolyesters were selected. Poly(3-hydroxybutyrate) (P(3HB)) is an optically active polyester which is stored in some bacteria as a source of energy [12,13,14,15]. By controlled fermentation, Imperial Chemical Ind. developed a procedure to produce copolyesters of hydroxybutyrate (HB) and hydroxyvalerate (HV) whose chemical structure is shown in fig. 1. P(3HB)-co-P(3HV) copolyesters are flexible random copolymers which for hydroxyvalerate (HV) molar ratios smaller than 30% crystallize in the P(3HB) unit cell. In this case HV units can be partially incorporated within the P(3HB) crystals [16] inducing a cocrystallization effect [16,17]. For HV molar ratios higher than 30% the chains adopt the P(3HV) unit cell [18]. Although the crystallization behaviour of these copolyesters has been extensively characterized [11,19,20] no attempt has been done so far to correlate microstructure with the dynamics of the amorphous phase during

crystallization in real time.

The aim of the present work is to establish a relationship between the change of the α-relaxation in flexible copolyesters and the restriction on the overall chain mobility imposed by the crystallization process. The study of the real time variation, in the frequency domain, of the shape parameters describing the dielectric relaxation of the α process upon crystallization allows a direct comparison with the predictions of different theoretical models.

2 Experimental Part

2.1 Dielectric Experiments

A series of P(3HB)-co-P(3HV) copolyesters having HB:HV molar ratios of 100:0, 94:6, 87:13, 78:22, and 74:26 were investigated. The copolymers were obtained from Zeneca Bio Products, U.K.. Number average, weight average molecular weight and polydispersity (M_n, M_w, and M_w/ M_n respectively) were calculated by Gel Permeation Chromatrography by using polystyrene standards and chloroform as solvent and are presented in table 1. In spite of the different nature of the copolyesters and the standard employed, the measured values are valid for comparative purposes. A nuclear magnetic resonance characterization confirmed the random nature of the copolymers and the HB:HV molar ratio. Semicrystalline films of $\approx 30\ \mu m$ in thickness were obtained by dissolving the

polymers in chloroform and subsequent casting at room temperature. Circular gold electrodes, 3 cm in diameter, were deposited onto the film surfaces by sputtering. Each film was placed on a home-made dielectric cell between two gold-plated stainless steel electrodes and introduced into a cryostat operating at a temperature controlled by a nitrogen atmosphere. Measurements of the complex dielectric permittivity ($\epsilon^* = \epsilon' - i\epsilon''$) were performed in the frequency range of 10^3 to 10^6 Hz using a Hewlett-Packard impedance analyzer HP 4192A. The dielectric measurements were made at constant temperature from -100° C to 100 ° C at 5° C steps. The error in temperature during the measuring time was estimated as ± 0.1 ° C. Amorphous specimens were obtained as follows: the solution cast sample was heated above its melting point. The sample was then pressed between two golden metallic blocks acting as electrodes in the subsequent dielectric experiment. Teflon spacers were used, both to control the sample thickness and to avoid short-circuit of the two electrodes. Under these conditions, the geometry of the samples cannot be estimated with enough accuracy to obtain absolute values of ϵ' and ϵ''. Therefore in this case only normalized values are presented. The sample was quenched between two cold blocks at T=0°C. The sample was finally placed in the dielectric cell at the selected measuring temperature. The time involved to achieve thermal stabilization in the sample was about 5 minutes. This gives rise to an error in

the initial time of crystallization of ± 2.5 min when comparing with the X-ray measurements.

According to the HN approach, eq. 1 can be used to derive the corresponding analytical expressions for the real and imaginary parts of the dielectric permittivity:

$$\epsilon' = (\epsilon_0 - \epsilon_\infty) r^{-c} cos(c\psi) + \epsilon_\infty \tag{2}$$

$$\epsilon'' = (\epsilon_0 - \epsilon_\infty) r^{-c} sin(c\psi) \tag{3}$$

with

$$r^2 = 1 + 2(\omega\tau_0)^b cos(b\pi/2) + (\omega\tau_0)^{2b} \tag{4}$$

and

$$tan\psi = \frac{(\omega\tau_0)^b sin(b\pi/2)}{1 + (\omega\tau_0)^b cos(b\pi/2)} \tag{5}$$

A subroutine based on Newton's method [4] was modified and used in the fitting. To estimate the uniqueness of the fitting parameters, their values were systematically varied and new fits were then obtained. We found that the maximum possible variation without provoking a significant deviation between the measured and calculated curves was less than $\pm 5\%$ for b, c and $\Delta\epsilon$, and $\pm 10\%$ for τ_0.

2.2 Real Time Wide Angle X-ray Scattering Experiments

Wide angle X-ray scattering (WAXS) experiments were performed by using a double-focusing mirror monochromator on the beam line A2 at HASYLAB (Hamburg, F.R.G.). The solution cast samples were heated in vacuum (10^{-2} torr). Thermal contact and homogeneous heating were ensured by a thin aluminum foil covering the surfaces of the film. The wavelength used was 0.15 nm. After melting of the sample, the selected crystallization temperature T_c was reached by cooling down the sample at a cooling rate of $\approx$ 40°C/min. WAXS patterns were recorded at selected accumulation times using a linear position-sensitive detector and corrected for fluctuations in the intensity of the primary beam and background.

3 Results

3.1 Wide angle X-ray scattering of the semicrystalline copolyesters.

X-ray scattering patterns of the investigated copolyesters at room temperature show the existence of well-defined Bragg maxima superimposed on an amorphous halo centered at about 2 nm^{-1} (fig. 2). The X-ray scattered intensity is represented as a function of the scattering vector s=$(2 \cdot sin\theta)/\lambda$ where 2θ is the scattering angle and is normalized to its maximum value. The position of the Bragg maxima corresponds to the orthorhombic PHB crystal lattice [11]. The

crystallinity of the samples was calculated using Vonk's method [11,21,22] as the ratio between the diffracted area under the deconvoluted crystalline peaks over the total diffracted area after subtraction of the continuous background. The shape of the amorphous halo due to the amorphous fraction was estimated from the diffraction pattern of the amorphous samples at temperatures above their melting points. With increasing HV content a slight decrease of the degree of crystallinity (X_c) from 0.67 for 100:0 to 0.45 for the 74:26 is observed (see table 1).

3.2 Dielectric relaxation of the semicrystalline copolyesters.

Dielectric loss (ϵ'') and dielectric constant (ϵ') values measured as a function of temperature at different frequencies for the semicrystalline samples are illustrated in figs. 3 and 4 respectively. Two main dielectric relaxations can be distinguished in the temperature range investigated: the α and the β relaxation in the order of decreasing temperature according to the criteria followed for semicrystalline polymers [1]. Both processes appear as maxima in ϵ'' and concurrent steps in ϵ'. The α process is prominent for all the investigated copolyesters while the β one appears as a faint shoulder at lower temperatures. For the 78:22 and 74:26 copolymers a magnification of the β relaxation is presented as an inset of fig. 3. For the sake of clarity only data at 10^3Hz

are included. Both, the α and β maxima move towards higher temperatures when the frequency is increased. Fig. 5 shows F_{max} values for both the α and the β relaxation as a function of the reciprocal temperature. The temperature dependence of the β process follows an Arrhenius behaviour with an activation energy of $\approx 13 \pm 1$ kcal/mol. On the contrary, the α process displays a curvature at the higher measured frequencies characteristic of a Vogel-Fulcher-Tamman dependence. The observed increment of the dielectric loss maximum at 10^6 Hz in fig. 3 may have two possible explainations by two facts. 1) It is known that in semicrystalline polymers the dielectric strength, $\Delta\epsilon$ of the α-relaxation can increase with temperature indicating a progressive mobilization of the amorphous phase [23,24,25]. Due to the fact that $\epsilon''_{max} \propto \Delta\epsilon$, then an increment of ϵ''_{max} with temperature is expected. 2) There is an additional source of increase in ϵ'' at 10^6 Hz which comes from the merging of the β with the α relaxation at high temperatures.

Fig. 6 represents the temperature of maximum loss for the α process at different frequencies for the investigated samples as a function of the HV content. An almost linear dependence of T_β on the HV molar composition is observed in the investigated HV concentration range. Moreover, the introduction of HV groups in the chemical structure of PHB tends to make the α relaxation narrower as depicted in fig. 7. Here normalized $\epsilon''/\epsilon''_{max}$ values corresponding

to the α relaxation have been represented versus the normalized frequency, F/F_{max}, for three selected cases. The relaxation curves were selected in order to have comparable central relaxation times τ_0 and therefore they correspond to different temperatures. The relaxation curves tend to become sharper with increasing amount of HV.

In P(3HB)-co-P(3HV) the β relaxation is expected to be mainly due to the contribution of the ester groups present in the main chain (see fig. 1) while the α-relaxation is related to segmental motions at T_g in accordance with previous dielectric studies [1,26,27,28].

3.3 Real time X-ray diffraction study during crystallization.

Figs. 8 and 9 illustrate the evolution of the WAXS patterns in real time during the isothermal crystallization of the 87:13 and 78:22 copolyesters respectively at T_c=30±0.2° C. The diffraction patterns were collected with an accumulation time of 0.5 and 1 min for 87:13 and 78:22 respectively. The X-ray scattered intensity is represented as a function of the reciprocal lattice vector s=$(2 \cdot sin\theta)/\lambda$. As crystallization time increases the reflexions 020 (s=1.48 nm^{-1}) and 110 (s= 1.86 nm^{-1}) which are characteristic of the orthorhombic PHB crystal lattice appear [11]. The contribution of the amorphous phase for every crystallization time was calculated by multiplying the initial scattering profile (

t_c=0) by a reduction factor and, then, shifting the obtained pattern along the s-axis till a good fit is achieved. The value of the degree of crystallinity is shown in fig. 10 for all the copolyesters investigated as a function of crystallization time t_c. As expected [29,30], during isothermal crystallization, after a certain induction time, X_c exhibits a rapid increase followed by a much slower process at longer times. In the case of the PHB homopolymer crystallization occurs so rapidly that under the present experimental conditions the sample crystallizes upon cooling. Both, the induction time and the final degree of crystallinity depend on the HV molar content. The higher the HV content the longer is the induction time and the lower is the final crystallinity value achieved in agreement with previous results [11].

3.4 Real time variation of the α relaxation process upon crystallization.

To investigate a crystallization process in real time one needs the measuring time to be shorter than the characteristic crystallization time. In particular, to follow in real time a crystallization process by dielectric spectroscopy fast measurements are required. In our case, at the measuring temperature of T=30°C the α relaxation process of the amorphous samples is centered around 10^4 Hz. The shape of the relaxation curve can be well described without interfering

with the kinetic process by measuring in the 10^3Hz<F<10^6Hz range [2]. This allows one to take data in 34 seconds.

Figs. 11 and 12 illustrate the real time evolution of the α-relaxation during an isothermal crystallization process at T_c=30±0.5° C for two selected copolyesters. Fig. 11a and 11 b show the ϵ'' and ϵ' data for the 87:13 copolyester. The data were normalized to the highest measured value. In fig. 11a every single curve shows the dependence of ϵ'' versus frequency for selected crystallization times. The initial curve, at t=0, corresponds to the amorphous polymer obtained as described in the experimental part. As crystallization proceeds two main features are observed. Firstly, there is a reduction of the intensity of the α-relaxation process as the crystallization time increases as characterized by the observed reduction of the ϵ'' maximum and the concurrent decrease of the step in ϵ'. Secondly, a shift of the frequency of the maximum loss, F_{max}, towards lower frequency values is detected for t>27 minutes. Figs. 12a and 12b show the ϵ'' and ϵ' data for the 78:22 copolyester in a similar fashion as for the previous figure. The variation of both, ϵ'' and ϵ' presents similar qualitatively features as those observed for the 87:13 copolymer with the only difference that the shift of F_{max} for the 78:22 copolymer is very small. A summary of the above results for the investigated copolyesters is presented in fig. 13a and 13b. The data for the 100:0 homopolymer are not included due to the fast kinetics of

crystallization of this sample (fig. 10). The crystallinity of 100:0 is 60% at t=0. Here, ϵ''_{max} and F_{max} values have been normalized by their initial values and are represented as a function of the crystallization time in a logarithmic scale. As shown in fig. 13a, there is a sigmoidal shape reduction of the normalized ϵ'' with time for all the investigated copolymers consisting on an initial plateau where almost no change of ϵ'' is observed. The extension in time of this first plateau depends on the HV molar content being longer for copolyesters with higher amounts of HV groups. Then, a sudden decrease of ϵ'' follows. Finally, ϵ'' levels off reaching a second plateau which exhibits a clear dependence on the HV molar content. The smaller the HV content the lower are the final ϵ'' values achieved. A rather different picture emerges from the inspection of fig. 13b. Here, only those samples with smaller amounts of HV, 94:6 and 87:13, exhibits a clear reduction of the F_{max} values during the crystallization process. On the contrary, for the copolyesters with higher amount of HV groups, 78:22 and 74:26, F_{max} exhibits almost no dependence with time. The observed difference between the behaviour with crystallization time exhibited by F_{max} depending on the HV molar content suggests a different slowing down of the overall chain mobility as crystallization occurs.

3.5 Phenomenological analysis of the dielectric data.

The phenomenological description of Havriliak-Negami (HN) for ϵ^* has been applied to the dielectric data shown in figs. 7, 11 and 12. The continuous lines in these figures correspond to the calculated fittings according to the HN equation (eq. 1) as previously described. The deviation of the experimental ϵ'' values at low frequencies from the calculated HN curve observed in fig. 11 might be due to the influence of dc conductivity. Table 2 shows the HN parameters for the semicrystalline copolyesters (fig. 7). In these cases, the α relaxation appears as a relative broad process as revealed by the b and c shape parameters. The HN parameters calculated for the isothermal crystallization experiments (fig. 11 and 12) are shown in fig.14 as a function of crystallization time. The sigmoidal-shape variation of the dielectric parameters presented in fig. 14 seems to follow the characteristic features of the isothermal crystallization process as shown in fig. 10. In particular, the total reduction of the dielectric strength (fig. 14a) depends on the amount of HV. The initial relaxation curves for the amorphous samples are asymmetric (c$\approx$0.5) and they present similar shape parameters. In all cases, as crystallization time increases a reduction of the asymmetry of the relaxation process, as denoted by an increase of the c parameter towards the highest possible value ($c = 1$), is observed. Additionally, a reduction of the b parameter revealing an increase of the broadening of the relaxation curves is

also detected. The normalized relaxation strength, $\Delta\epsilon$, suffers a clear decrease at earlier stages of crystallization and it levels off at longer crystallization times. The central relaxation time τ_0, first, slightly decreases for short crystallization times and then, for the 87:13 and 94:6 copolymers, bends upwards while it remains at a constant level for the other copolymers. It is worth to mention that at the early stages of crystallization the relaxation time distribution function is not symmetric ($c \neq 1$, fig. 14c). In this case τ_0 differs from the average relaxation time, $< \tau >$.

4 Discussion.

4.1 Dielectric Relaxation of the Semicrystalline copolyesters.

The introduction of HV units in the polymer backbone of P(3HB) induces a reduction in the overall degree of crystallinity by almost a 20% (see table 1) in accordance with previous studies [11]. As in most semicrystalline polymers with high crystallinity , the calorimetric T_g of PHB-co-PHV copolymers is difficult to be distinguished [31]. In these cases dilatometric [31] or relaxation techniques are needed [23,24,31]. Dielectric relaxation measurements can be very helpful to define a dynamic $T_g(F)$, as the temperature at which the maximum value of the dielectric loss occurs at a given frequency F [23,24]. Calorimetric and dynamic mechanical measurements [28,31,32,33], have shown that the

α relaxation of the P(3HB)-co-P(3HV) copolyesters can be attributed to the large scale motions appearing at the glass transition temperature. Thus, we can identify $T_g(F)=T_\alpha(F)$. The presence of HV units in the polymeric chain of P(3HB) produce a softening of the polymer as revealed by the decrease of T_α with increasing HV molar content (fig. 6). This effect mimics the dependence followed by both, melting temperatures and enthalpies of fusion reported for P(3HB)-co-P(3HV) copolyesters [11,18]. As shown in fig. 7, the presence of HV units in the structure of PHB results in a narrowing in the α relaxation characterized by the observed increase of the b parameter. The influence of crystallinity on the shape of the α-relaxation has been investigated by several authors [1,2,3,4,10]. In polymeric amorphous systems the α-relaxation is generally asymmetric. The presence of crystals produces a broadening and a symmetrization of the relaxation. In our case, the investigated semicrystalline copolymers (fig. 7) seem to follow the above mentioned features. The higher the degree of crystallinity the broader and more symmetric is the relaxation process as revealed by the reduction of the b-parameter and the concurrent increase of the c-parameter (table 2).

The subglass β relaxation in P(3HB)-co-P(3HV) copolyesters can be associated to a local motion of the ester groups [1,27,26,28]. As compared with more rigid polyesters, like PET, in P(3HB)-co-P(3HV) copolymers the β relaxation

is relatively weak in relation to the α one. Due to the high flexibility of these copolyesters the glass transition appears at lower temperatures than in PET, masking the subglass process. Additionally, in P(3HB)-co-P(3HV) copolymers a weaker β relaxation is expected due to the fact that there is a single dipolar ester group per monomeric unit while in PET there are two ester groups.

4.2 Influence of the microstructure on the molecular mobility.

It is known that P(3HB)-co-P(3HV) copolymers crystallize forming spherulites [34]. For these copolymers, the real time crystallinity variation obtained from WAXS isothermally presents a typical sigmoidal shape (fig. 10). The first rapid X_c increase can be attributed to a primary crystallization process where the amorphous phase is being filled with spherulites [11,30]. As spherulites impinge with each other, and fill up the sample a much slower secondary crystallization starts characterized by a leveling off of X_c. The final degree of crystallinity is a function of the HV molar content. In the molar range investigated the copolymers crystallize in the P(3HB) crystal lattice [11,34]. As ethyl side chains of the HV units disturb the crystallization on the P(3HB) lattice the overall crystallinity is reduced with the increasing of HV content [11].

Similarly to the case of semirigid polymers (PET [2,10,35] and PEKK [4]), the development of crystallinity during crystallization in P(3HB)-co-P(3HV)

copolymers reduces the intensity of the α-relaxation (fig. 13a) as polymeric segments are progressively immobilized when they incorporate the crystals. As crystallization proceeds, a slowing down of the remaining amorphous phase is observed for the 94:6 and 87:13 copolymers as revealed by the decrease of the F_{max} values (fig. 13b). This effect has been attributed to the confinement of the amorphous polymer phase between the crystalline regions giving rise to a reduction of the overall mobility [1]. Surprisingly, 78:22 and 74:26 copolymers do not exhibit any change of F_{max} with crystallization time. The fact that the HV molar content included in the crystalline phase is smaller than the overall HV molar amount is well documented [16]. As crystallization occurs an enrichment in HV units of the amorphous phase is expected. This effect does not modify significantly the dynamics of the α relaxation. Indeed, according to our dielectric measurements, regardless of the HV concentration, all the amorphous systems present similar values of the shape parameters (fig. 14). Moreover, in the investigated HV range, similar F_{max} values for the amorphous samples, before crystallization, are obtained (fig. 13). From this result we conclude that the variation of the HV concentration of the amorphous phase as crystallization proceeds does not seem to be responsible for the different behaviour shown in fig. 13b.

One could attribute the different behaviour of F_{max} as a function of t_c to the

decrease of the degree of crystallinity depending on HV molar content. However, it is worth mentioning that while the final crystallinity of 87:13 and 78:22 is very similar ($\approx$ 37 %), F_{max} behaves in a completely different manner (see fig. 13b). The different degree of restriction of the amorphous phase between the two copolyesters with similar degrees of crystallinity can be , therefore, attributed to the microstructure. Structural models have been recently presented for spherulitic filling systems [36,37,38], including P(3HB)-co-P(3HV) copolymers [39]. These models propose an inhomogeneous distribution of lamellar stacks within the spherulites. It has been shown that the microstructure of semirigid polymers like PET and some poly(aryl ether ketone)s may present the existence of amorphous gaps between lamellar stacks [36,38] or even of broad amorphous regions (liquid pockets) [37]. It has been reported that as the amount of HV increases, the steric hindrance induced by the HV groups leads to thinner lamellar crystals [39] which arrange in more imperfect spherulites [20]. Our results can be explained assuming that, in one hand, compact spherulites, like those of 87:13 and 94:6, give rise to a homogeneous distribution of lamellar stacks with small amorphous gaps between them. Here, the amorphous phase is highly restricted and, therefore, these copolymers show the observed decrease of F_{max} with crystallization time. On the other hand, copolymers with high amount of HV groups, like 78:22 and 74:26, organize themselves in looser

spherulites [20] where restrictions are expected to be weaker and no variation of F_{max} is detected.

It is to be noted that PET and PEKK having similar, or even smaller, degree of crystallinity than that achieved by 78:22 and 74:26 exhibit the slowing down effect characterized by a decrease of F_{max} with increasing crystallinity [1,4]. As mentioned above, these systems present loose spherulites [37]. Thus, the different level of F_{max} slowing down observed for the 78:22 and 74:26 copolyesters and PET and PEKK can be attributed to the different chain flexibility between P(3HB)-co-P(3HV) copolyesters and the more rigid PET and PEKK ones.

4.3 Correlation of dielectric strength and microstructure.

Additional information can be gained from the parallel study of the evolution of the dielectric strength as a function of crystallinity as shown in fig. 15. Since $\Delta\epsilon$ is proportional to the density of free dipoles involved in the α-relaxation [26], the decrease of $\Delta\epsilon$ with crystallinity can be associated with a progressive reduction of the amorphous phase as segments of the polymeric chains are gradually incorporated within the crystals. The reduction of the mobile fraction on the basis of the $\Delta\epsilon$ decrease is about 70 % for 87:13 to a 60% for 78:22. However, the amorphous phase on the basis of the final crystallinity values suffers a decrease of $\approx$37% for both 87:13 and 78:22. This finding suggests that there exists an

excess of immobile material in addition to that included in the crystals. Similar observations have been reported in PET [1,2], PEEK [23,24] and PEKK [4,25] among others. The existence of a rigid amorphous phase has been proposed in semirigid polymers [40]. This rigid amorphous phase appears as a consequence of constrains of the semi-rigid amorphous chains provoked by the influence of the crystal lamellae upon crystallization under highly restrictive conditions [40]. These conditions include fast crystallization from the melt state or low cold-crystallization temperatures.

Combination of calorimetric and X-ray experiments indicates that the material in interlamellar amorphous regions has a very low degree of mobility as compared with that located in amorphous gaps between lamellar stacks [36]. In addition, the plot of $\Delta\epsilon$ versus crystallinity (fig. 15) indicates that for similar crystallinity the amount of immobile material is similar regardless of the HV content. The origin of this immobile material has to be sought in the lamellar stacks i.e. not only in the crystalline lamella but also in the interlamellar amorphous region. Thus, for a given amount of lamellar stacks, controlling the crystallinity, the amount of immobile material does not depend on the distribution of these stacks. However, as mentioned above, the amorphous material located in the interstack amorphous gaps may exhibit a different level of mobility depending on the homogeneity of the distribution of the stacks.

For the sake of comparison $\Delta\epsilon$ values for PEKK [4] have been presented in fig. 15. In this case a weaker dependence of $\Delta\epsilon$ with crystallinity is observed which may be attributed to differences in the microstructure. These results point towards the fact that, a discussion on the relationship between microstructure and dynamics of systems with varying flexibility needs additional structural information to that given by the crystallinity. In addition, similarly to PEKK [25] and PEEK [40] the effect of crystallization at higher temperatures, i.e. less restrictive conditions, could also affect the overall amount of immobile amorphous material. Efforts towards a deeper knowledge on the correlation between microstructure and dynamics are in progress.

4.4 Distribution of relaxation times during the crystallization process

The observed evolution of the shape parameter b and c for the α relaxation process with crystallization time indicates that the relaxation time distribution function broadens and becomes more symmetric. This is a general trend followed by a great variety of polymers [1,4,10,41]. As crystallinity increases restrictions to the available possible conformations appear [1]. Segments of the polymeric chains included in the crystals hinder the overall mobility of bonded segments. This affects large, rather than small scale motions. As for previ-

ously investigated polymers the Schlosser and Schönhals model can be used to interpret these results. The observed decrease of b could be interpreted as due to an increasing hindrance for large scale motions as crystallization occurs and the system is being progressively covered by spherulites. On the other hand, as derived from fig. 14, the value of the product $b \cdot c$ does not change significantly. This would imply that small scale motions are less affected by the crystallization process.

5 Conclusions

Dielectric methods can be used to characterize the changes occurring in P(3HB)-co-P(3HV) flexible copolyesters during isothermal crystallization in real time. Similar to systems of lower flexibility, the variation of the dielectric parameters follows a sigmoidal-shaped pattern characteristic of an isothermal crystallization process of a polymer. The measured maximum loss frequency decreases with crystallization time suggesting a progressive reduction of the overall mobility of the polymeric chains as the system becomes more crystalline. The degree of slowing down depends on HV molar content. This effect has been explained by considering that the smaller the amount of HV units the more compact spherulites can be formed. The observed reduction of the mobile fraction as deduced by the decrease of the dielectric strength cannot be exclusively

explained on the basis of the amount of crystalline material. Our results can be explained by assuming an almost absence of mobility in the interlamellar amorphous regions. The mobile material is essentially located on the amorphous gaps between lamellar stacks. By comparing the results of the P(3HB)-co-P(3HV) copolyesters with more rigid polymers the influence of chain flexibility on the crystalline induced restrictions has been discussed. The smaller the flexibility the more effective seems to be the restriction suffered by the amorphous phase.

Acknowledgments.

The authors are indebted to the DGICYT (grant PB 94-0049), Spain, and to NEDO's International Joint Research Program, Japan for generous support of this investigation. We thank Dr. P.A. Barker and Dr. J.J. Liggat for providing the samples. A.N. thanks the support from the FPI program of the Spanish Ministry of Science. The experiments at HASYLAB (Hamburg, Germany) have been funded by the program Human Capital and Mobility, Access to large Instalations EC.

References

[1] J.C. Coburn, R.H. Boyd, Macromolecules **19**, 2238 (1986).

[2] G. Williams, Adv. Polym. Sci. **33**, 59 (1979).

[3] E. Schlosser, A. Schönhals, Colloid & Polymer Sci. **267**, 963 (1989).

[4] T.A. Ezquerra, J. Majszczyk, F.J. Baltà-Calleja, R. López-Cabarcos, K.H. Gardner, B.S. Hsiao, Phys. Rev. B **50**, 6023 (1994).

[5] J. Dobbertin, A. Hensel, C. Schick, J. Thermal Anal. **47**, 1027 (1996)

[6] S. Havriliak, S. Negami, Polymer **8**, 161 (1967).

[7] A. Schönhals, E. Schlosser, Colloid & Polym. Sci. **267**, 125 (1989).

[8] A. Schönhals, F. Kremer, E. Schlosser, Phys. Rev. Lett. **67**, 999 (1991).

[9] T.A. Ezquerra, Z. Roslaniec, E. López-Cabarcos, F.J. Baltà-Calleja, Macromolecules **28**, 4516 (1995).

[10] T.A. Ezquerra, F.J. Baltá-Calleja, H.G. Zachmann, Polymer **35**, 2600 (1994).

[11] M. Kunioka, A. Tamaki, Y. Doi, Macromolecules **22**, 694 (1989).

[12] R. Sharma, A.R. Ray, J.M.S.-Rev. Macromol. Chem. Phys. **C35(2)**, 327 (1995).

[13] T. Tanio, T. Fukui, Y. Shirakura, T. Saito, K. Tomita, T. Kahio, S. Masamune, J. Biochem. **124**, 71 (1982).

[14] P.A. Holmes, Developments in Crystalline Polymers-2, Ed. D.C. Basset, Elsevier Appl. Sci. Publ. ltd.: Amsterdam, 1988, p 1.

[15] L.I. Young, E.M. Stegantseva, L. Savenkova, Y.H. Park, J. of Microbiol. and Biotechnol. **100**, 5 (1995).

[16] D.L. VanderHart, W.J. Orts, R.H. Marchessault, Macromolecules **28**, 6394 (1995).

[17] N. Kamiya, M. Sakurai, Y. Inoue, R. Chujo, Y. Doi, Macromolecules **24** 2178 (1991).

[18] T.L. Bluhm, G.K. Hamer, R.H. Marchessault, C.A. Fyfe, R.P. Veregin, Macromolecules **19**, 2871 (1986).

[19] H. Mitomo, P.J. Barham, A. Keller, Polym. J. **19**, 1241 (1987).

[20] S.J. Organ, P.J. Barham, J. of Mat. Sci. **26**, 1368 (1991).

[21] F.J. Baltá-Calleja, C.G. Vonk, X-ray Scattering of Synthetic Polymers, Elsevier Amsterdam (1989).

[22] D.J. Blundell, B.N. Osborn, Polymer **24**, 953 (1983).

[23] P. Huo, P. Cebe, Macromolecules **25**, 902 (1992).

[24] D.S. Kalika, R.K. Krishnaswamy, Macromolecules **26** , 4252 (1993).

[25] R.K. Krishnaswamy, D.S. Kalika, Polymer **37**, 1915 (1996).

[26] P. Hedvig, Dielectric Spectroscopy of Polymers, Adam Hilger Ltd. Bristol (1977).

[27] Y. Ando, E. Fukada, J. of Polym. Sci.:Polym. Phys. Ed. **22**, 1821 (1984).

[28] F. Biddlestone, A. Harris, J.N. Hay, T. Hammond, Polymer International **39**, 221 (1996).

[29] J.M. Schultz, Polymer Materials Science, Prentice Hall: N.Y. 1974.

[30] H.G. Zachmann, C. Wutz, Crystallization of Polymers, Ed. by M. Dosière, Kluwer Academic Publishers Dordrecht (1993).

[31] P.J. Barham, A. Keller, E.L. Otun, P.A. Holmes, J. of Mat. Sci. **19**, 2781 (1984).

[32] M. Avella, B. Immirzi, M. Malinconico, E. Martuscelli, M.G. Volpe, Polymer International **39**, 191 (1996).

[33] G.J.M. de Koning, PhD. Thesis, Technical University Eindhoven, The Netherlands, **1993**.

[34] P.J. Barham, Materials Science and Technology vol 12: Structure and Properties of Polymers, Ed. by R.W. Cahn, P. Haasen, E.J. Kramer, VCH Weinheim (1993).

[35] K. Sawada, Y. Ishida, J. Polym. Sci., Part A-2 **13**, 2247 (1975).

[36] B.B. Sauer, B.S. Hsiao, Polymer **36**, 2553 (1995).

[37] R. Verma, H. Marand, B. Hsiao, Macromolecules **29**, 7767 (1996).

[38] C. Santa Cruz, N. Stribeck, H.G. Zachmann, F.J. Baltá-Calleja, Macromolecules **24**, 5980 (1991).

[39] R.J. Rule, J.J. Liggat, Polymer **36**, 3831 (1995).

[40] S.Z.D. Cheng, M.Y. Cao, B. Wunderlich, Macromolecules **19**, 1868 (1986).

[41] G. Williams, Materials Science and Technology vol 12: Structure and Properties of Polymers, Ed. by R.W. Cahn, P. Haasen P., E.J. Kramer, VCH Weinheim (1993).

Table 1: Characterization of P(3HB)-co-P(3HV) copolyesters.

$HB:HV$	100:0	94:6	87:13	78:22	74:26
Mn (10^3 g/mol)	152	161	183	234	217
Mw (10^3 g/mol)	345	387	371	428	403
Mw/Mn	2.3	2.4	2.0	1.8	1.9
X_c	0.67	0.67	0.56	0.41	0.45

Table 2: HV:HB, $\Delta\epsilon$; b, c *and* τ_0 obtained from the fitting of equations 1 for the α-relaxation data shown in fig. 7.

HV:HB	$\Delta\epsilon$	b	c	τ_0(s)	T(°C)
87:13	1.83	0.32	1	$7.8 \cdot 10^{-6}$	40.5
78:22	1.47	0.4	1	$5 \cdot 10^{-6}$	31.1
74:26	1.86	0.56	0.71	$7.8 \cdot 10^{-6}$	30.1

Legends to the figures.

Figure 1: Chemical structure of P(3HB)-co-P(3HV)

Figure 2: WAXS diffractograms of the semicrystalline P(3HB)-co-P(3HV) copolyesters prepared by solution cast obtained at 30 °C .

Figure 3: Isochronal ϵ'' for the solution cast semicrystalline samples as a function of temperature. Measuring frequencies: 10^3(o), 10^4(•), 10^5(△), 10^6(▲) Hz. The insets for the 78:22 and 74:26 copolymers present a magnification of the β relaxation.

Figure 4: Isochronal ϵ' for the solution cast semicrystalline samples as a function of temperature. Same symbols as in Fig.3.

Figure 5: Log[F_{max}] as a function of the reciprocal temperature for PHB-co-PHV copolymers:100:0 •, 94:6 ■, 87:13o, 78:22 □, 74:26 △. The continuous lines are a guide for the eye.

Figure 6: Temperature of maximum loss for the α process at different frequencies for P(3HB)-co-P(3HV) as a function of HV content. Same symbols as in fig. 3.

Figure 7: Normalized $\epsilon''/\epsilon''_{max}$ ratio versus Log (F/F_{max}) for: o 87:13 (40.5 °C) ; □ 78:22 (31.1 ° C) and △ 74:26 (30.1 °C) copolyesters. The relaxation curves were selected to display similar τ_0 values (see table 2). The continuous lines are HN fits according to eq. 1. Fitting parameters are shown in table 2

Figure 8: Real time WAXS patterns, as a function of s=$(2 \cdot sin\theta)/\lambda$, taken at selected crystallization times at T=30 °C of the 87:13 copolyester. The contribution of the amorphous and crystalline phases at every crystallization time is represented by the dotted lines.

Figure 9: Real time WAXS patterns, as a function of s=$(2 \cdot sin\theta)/\lambda$, taken at selected crystallization times at T=30 °C of the 78:22 copolyester. The contribution of the amorphous and crystalline phases at every crystallization time is represented by the dotted lines.

Figure 10: Time dependence of the X-ray crystallinity for the copolyesters investigated: 100:0 •, 94:6 ■, 87:13o, 78:22 □, 74:26 △.

Figure 11: Real time evolution of normalized $\frac{\epsilon''}{\epsilon''_{max}}$(a) and normalized $\frac{\epsilon'_{max}}{\epsilon'_{max}}$ (b) versus frequency for the 87:13 copolymer during an isothermal crystallization process at T=30±0.5°C at selected crystallization times in minutes. Both ϵ''_{max} and ϵ'_{max} are the maximum measured values. The continuous lines are HN fits according to eq. 1. Fitting parameters are shown in fig. 14

Figure 12: Real time evolution of normalized $\frac{\epsilon''}{\epsilon''_{max}}$ (a) and normalized $\frac{\epsilon'}{\epsilon'_{max}}$(b) versus frequency for the 78:22 copolymer during an isothermal crystallization process at T=30±0.5°C at selected crystallization times. Both ϵ''_{max} and ϵ'_{max} are the maximum measured values. The continuous lines are HN fits according to eq. 1. Fitting parameters are shown in fig.14

Figure 13: (a) Relative variation of the maximum dielectric loss values, $\frac{\epsilon''_{max}(t)}{\epsilon''_{max}(0)}$ and (b) variation of the frequency of maximum loss values, F_{max}, as a function of the crystallization time for the investigated copolyesters. Same symbols as in fig. 10.

Figure 14: Real time evolution of the normalized $\Delta\epsilon$, b and c and central relaxation time τ_0 during the isothermal crystallization process for the investigated copolyesters. Same symbols as in fig. 10. Continuous lines are guides for the eyes

Figure 15: Normalized $\Delta\epsilon$ as a function of crystallinity for: 74:26 $\triangle$, 78:22 $\square$ and 87:13 o. Data for PEKK ($\blacktriangle$) are taken from ref. 4. Continuous lines are guides for the eyes

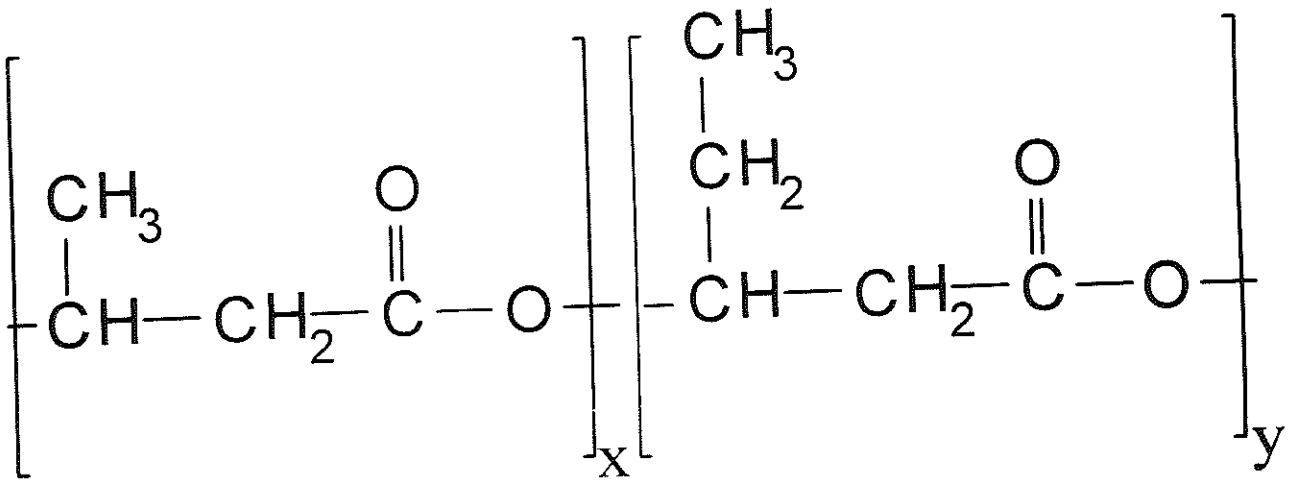

Fig.1

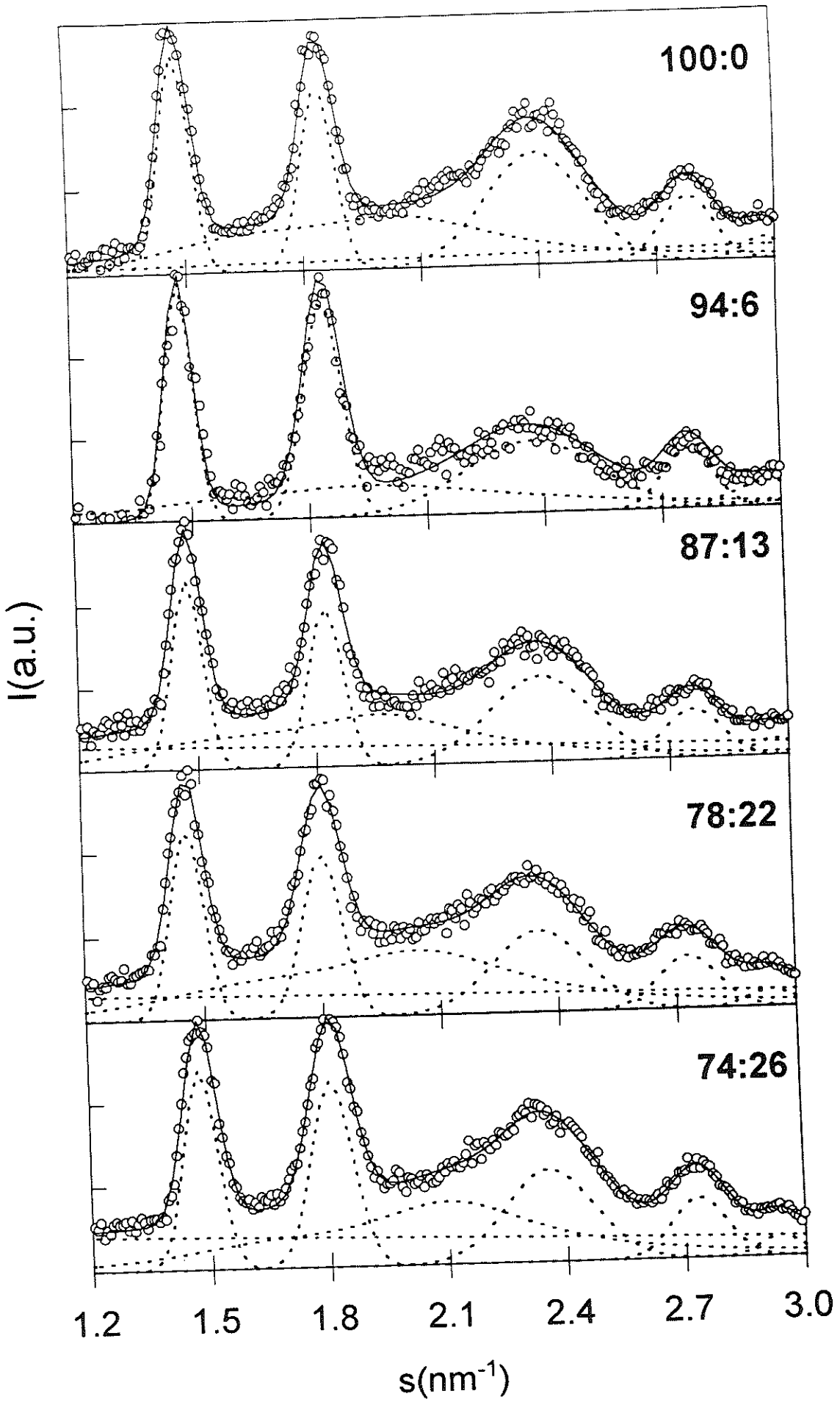

Fig. 2

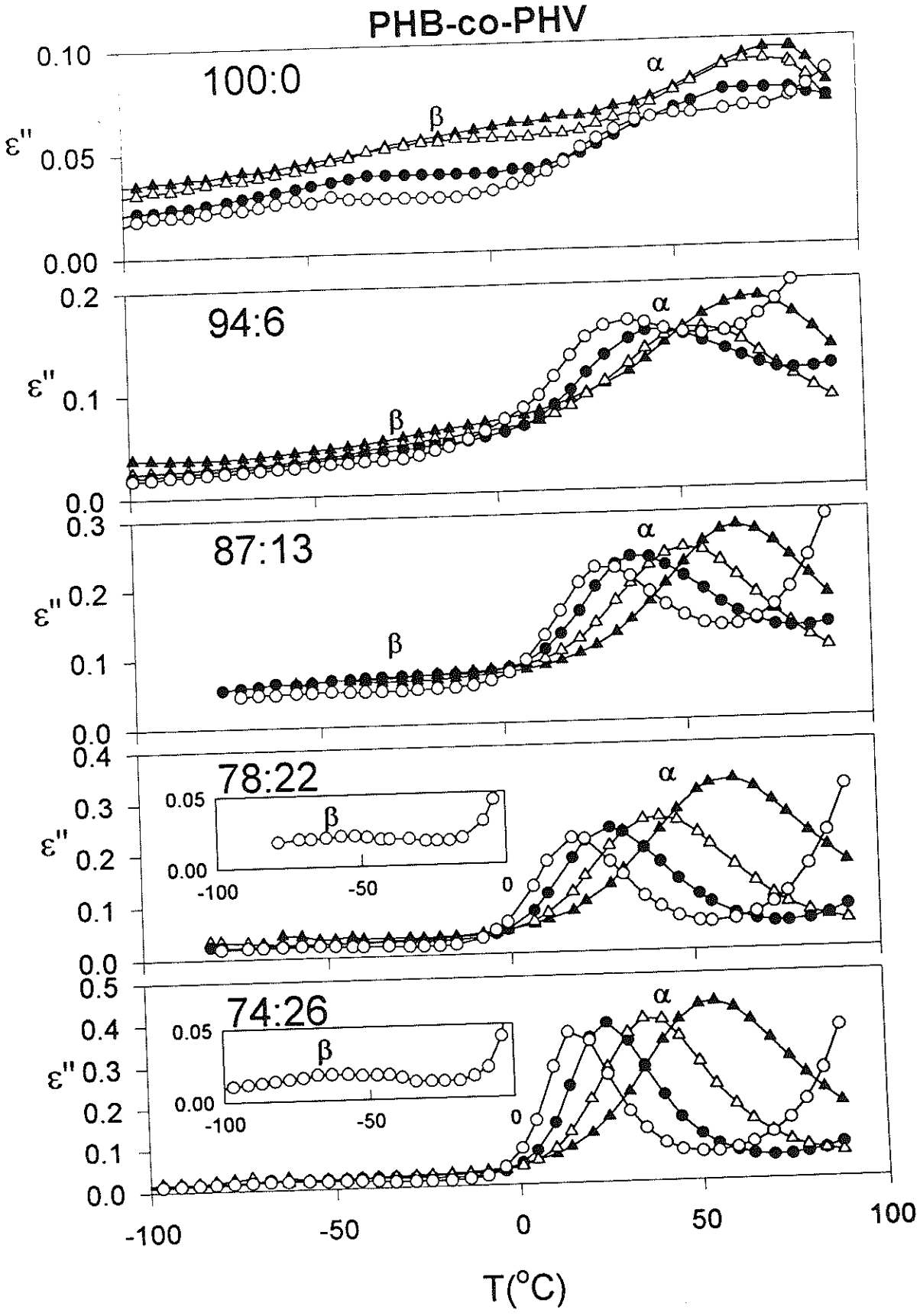

Fig. 3

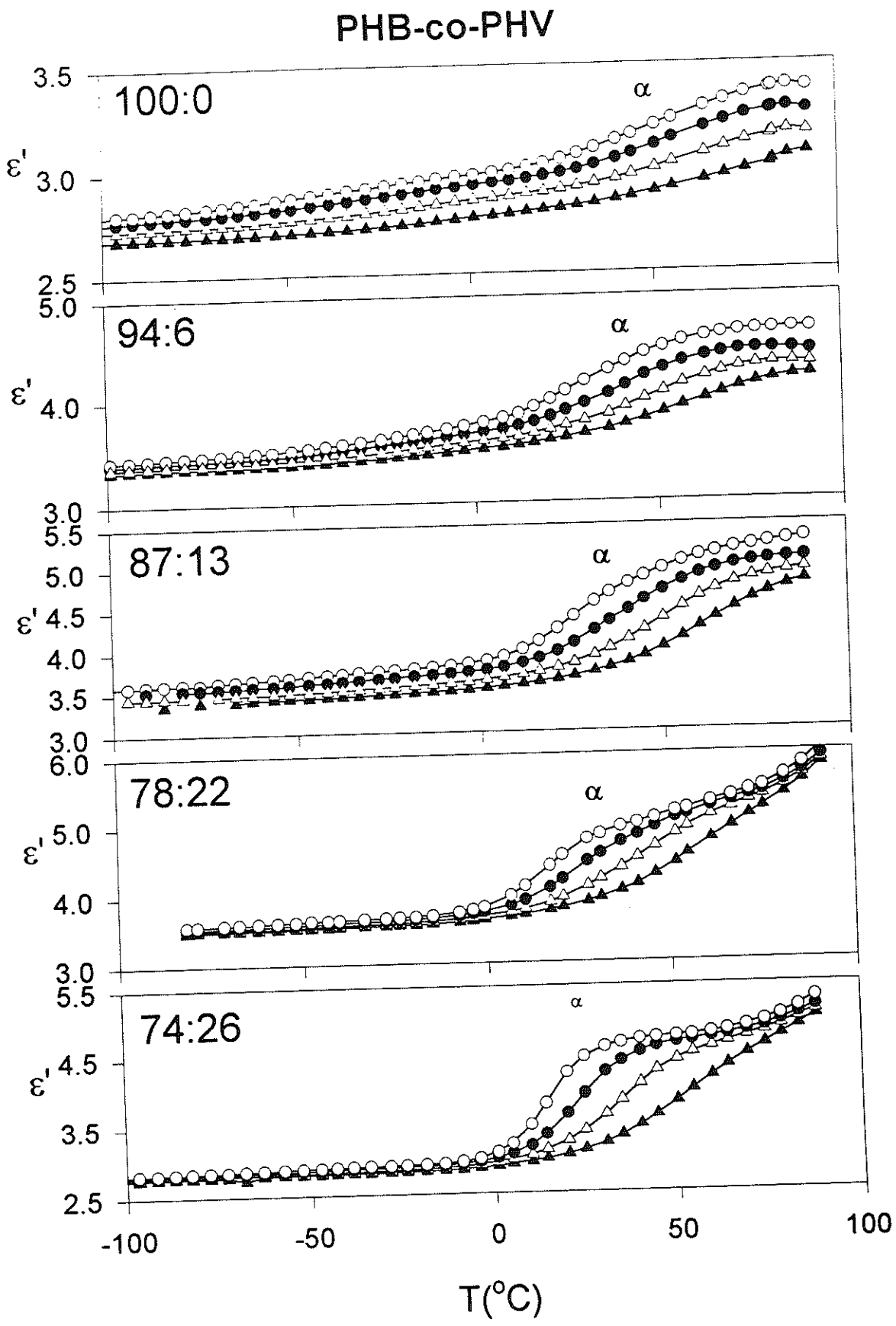
PHB-co-PHV
100:0
94:6
87:13
78:22
74:26
α
ε'
3.5
3.0
2.5
5.0
4.0
5.5
4.5
6.0
-100
-50
0
50
100
T(°C)

Fig. 4

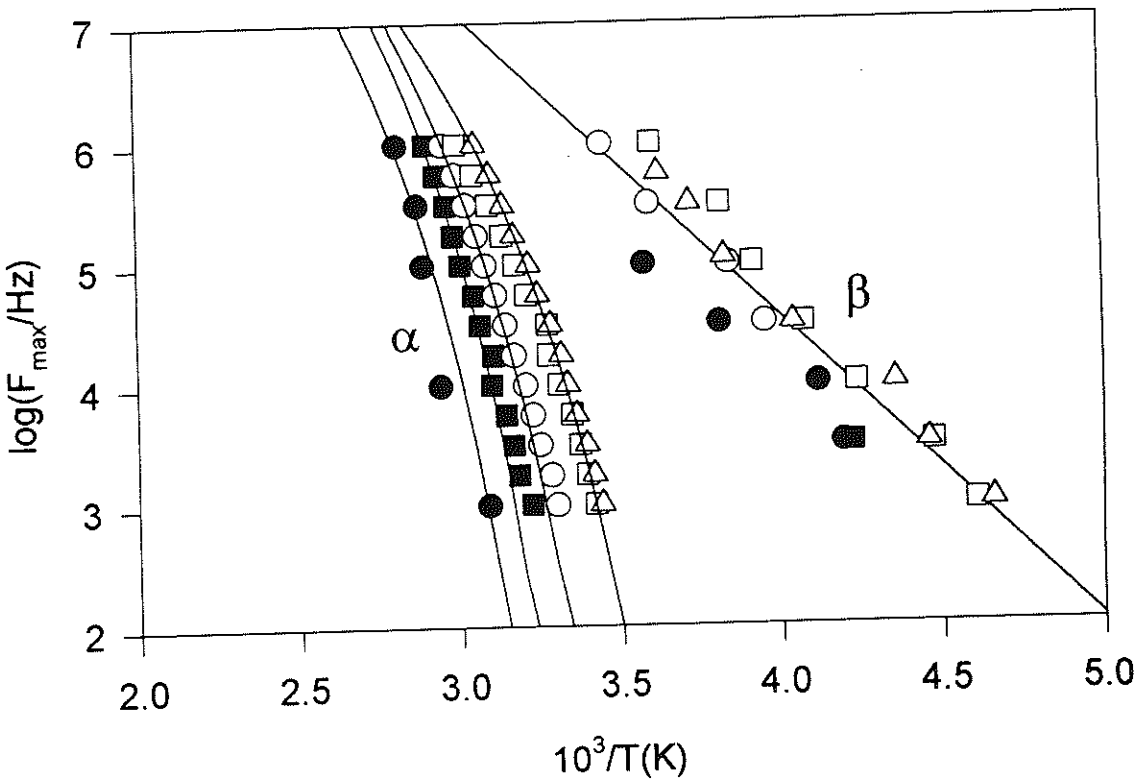

Fig. 5

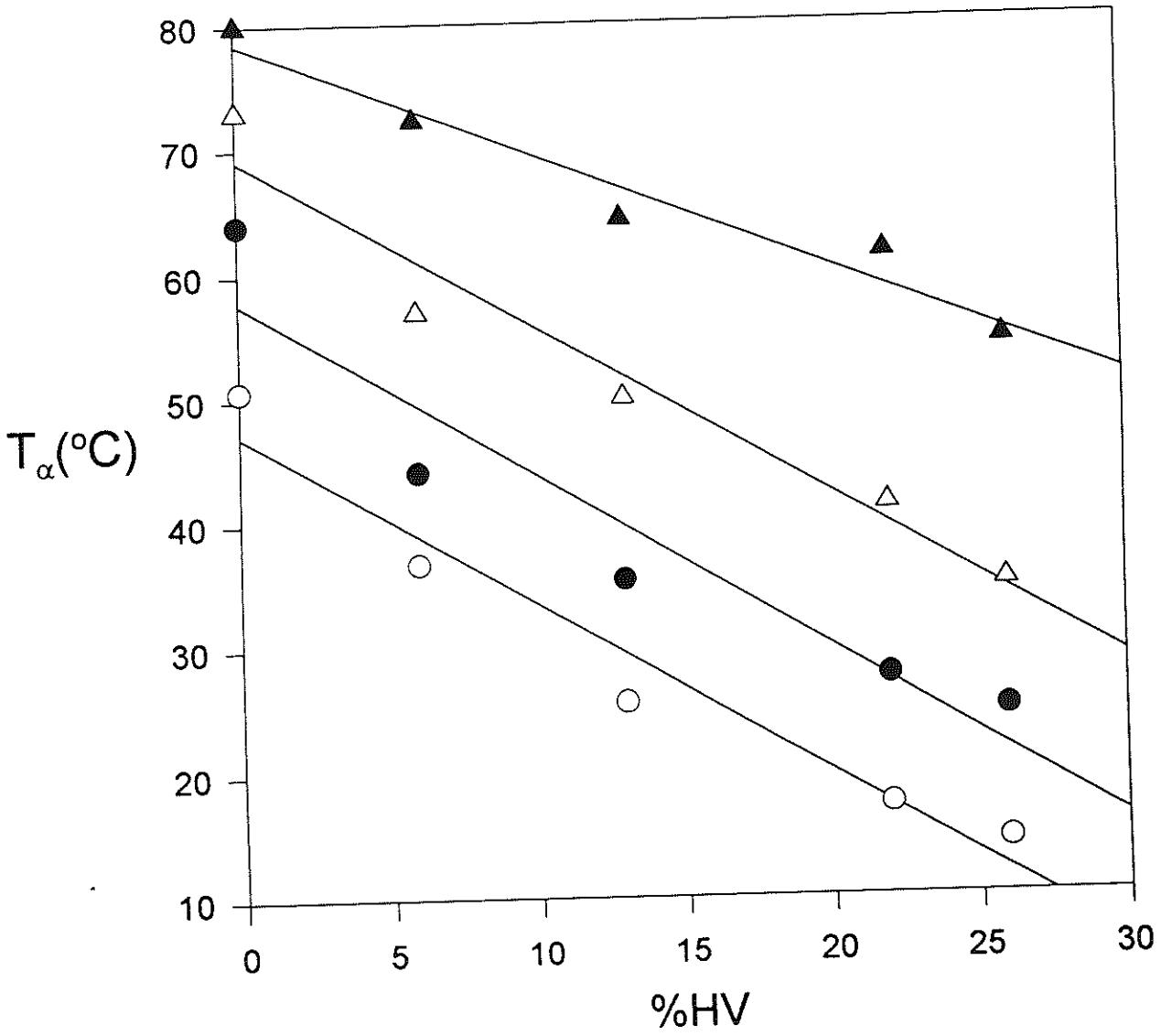

Fig. 6

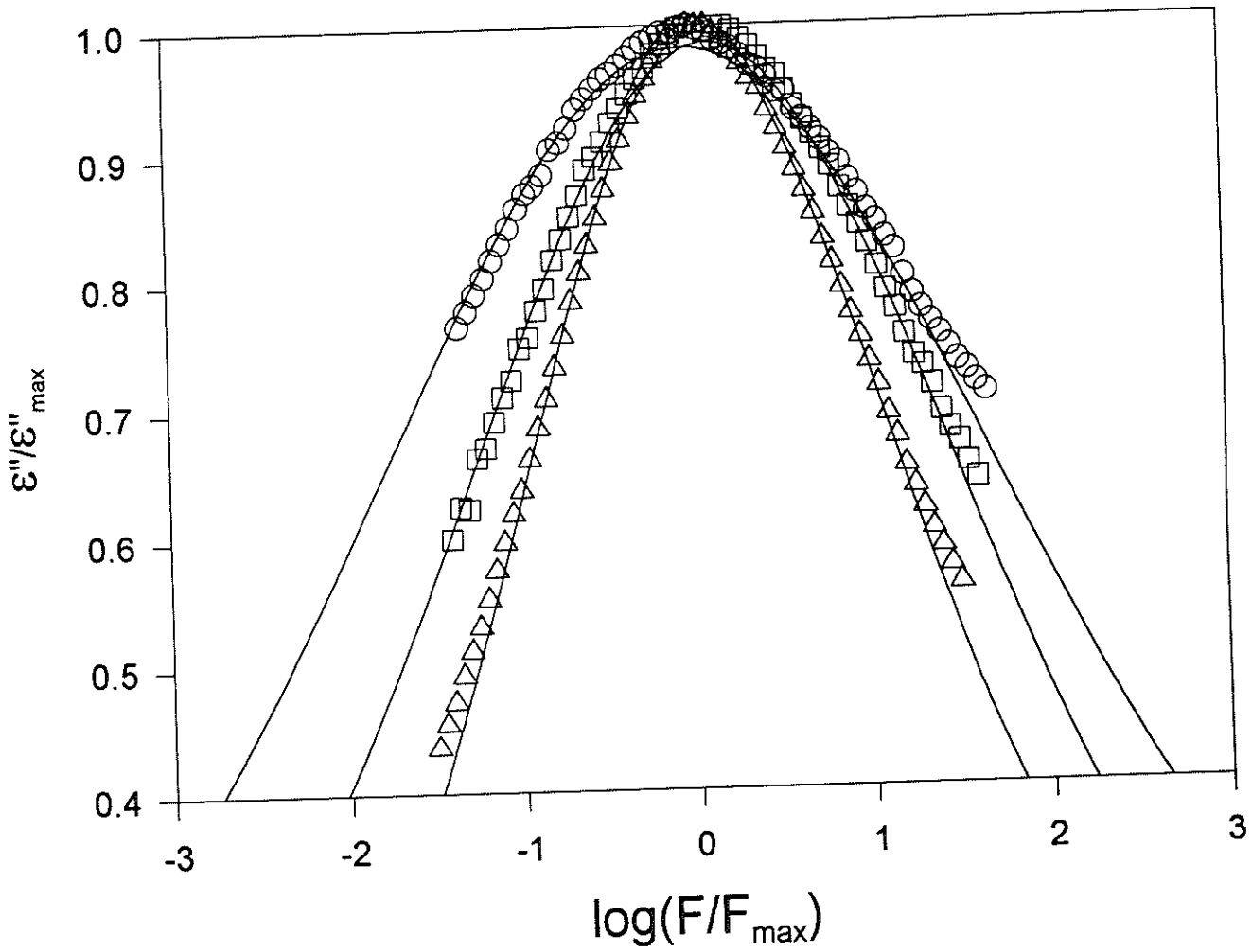

Fig.7

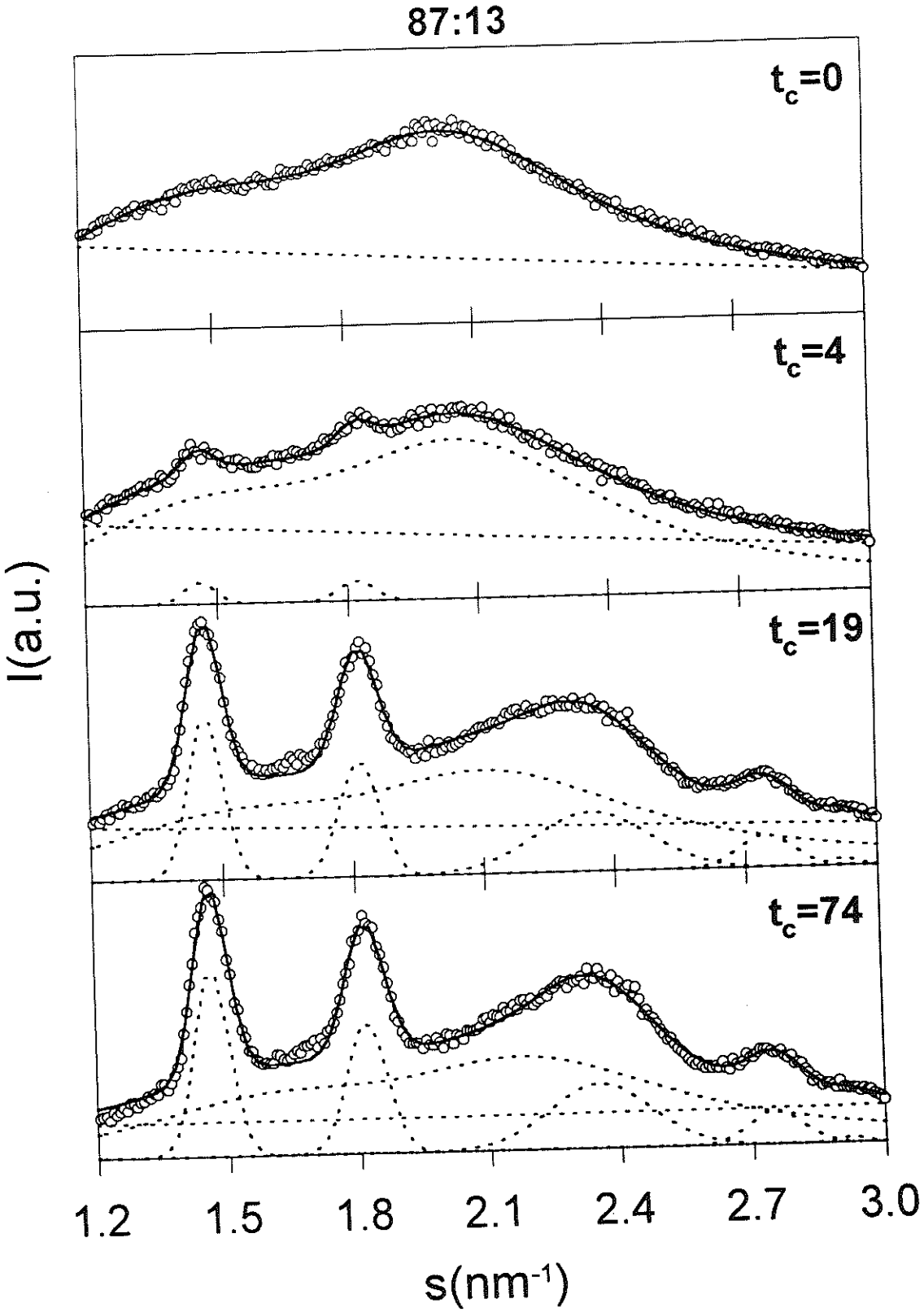

Fig.8

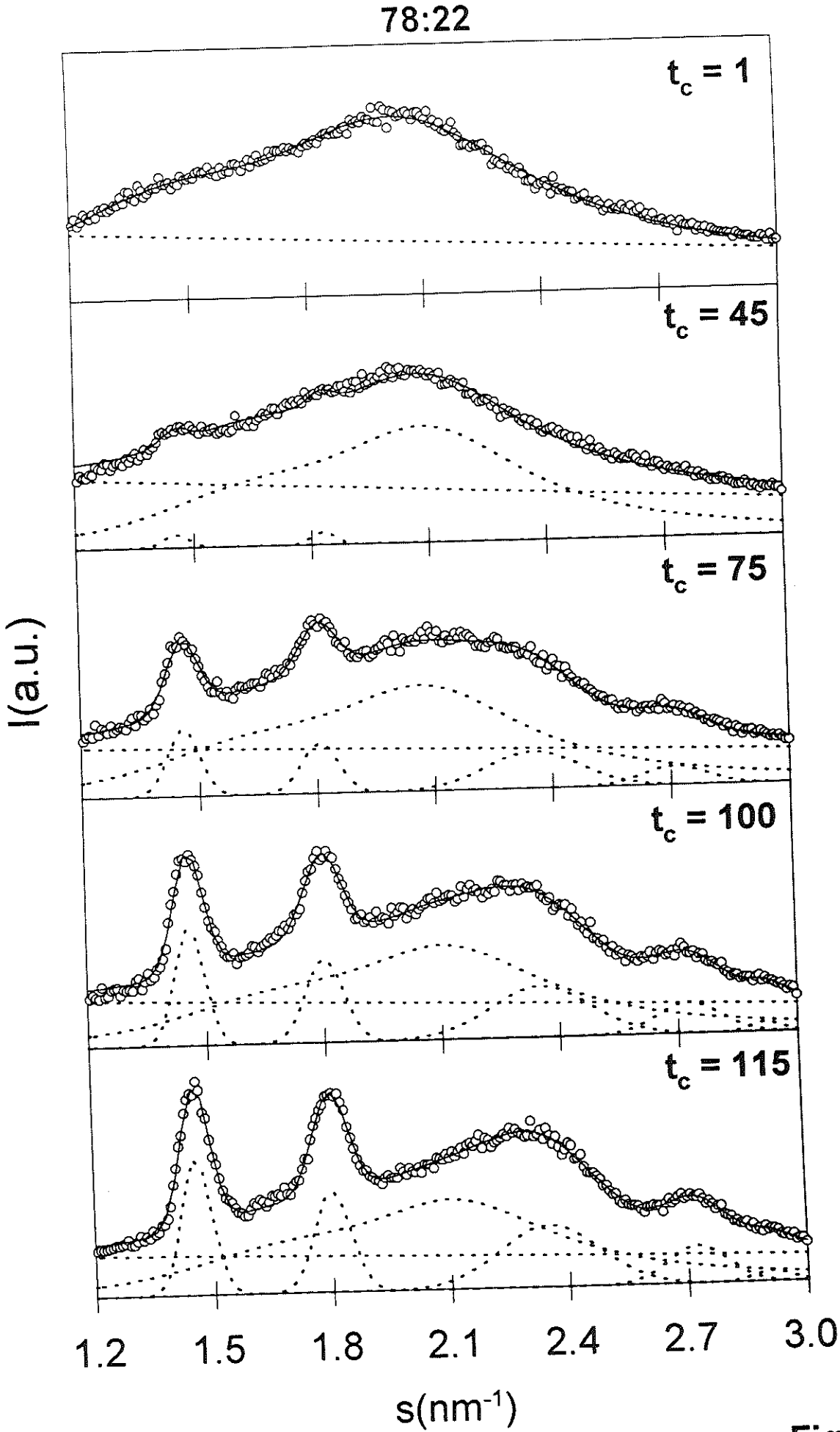

Fig.9

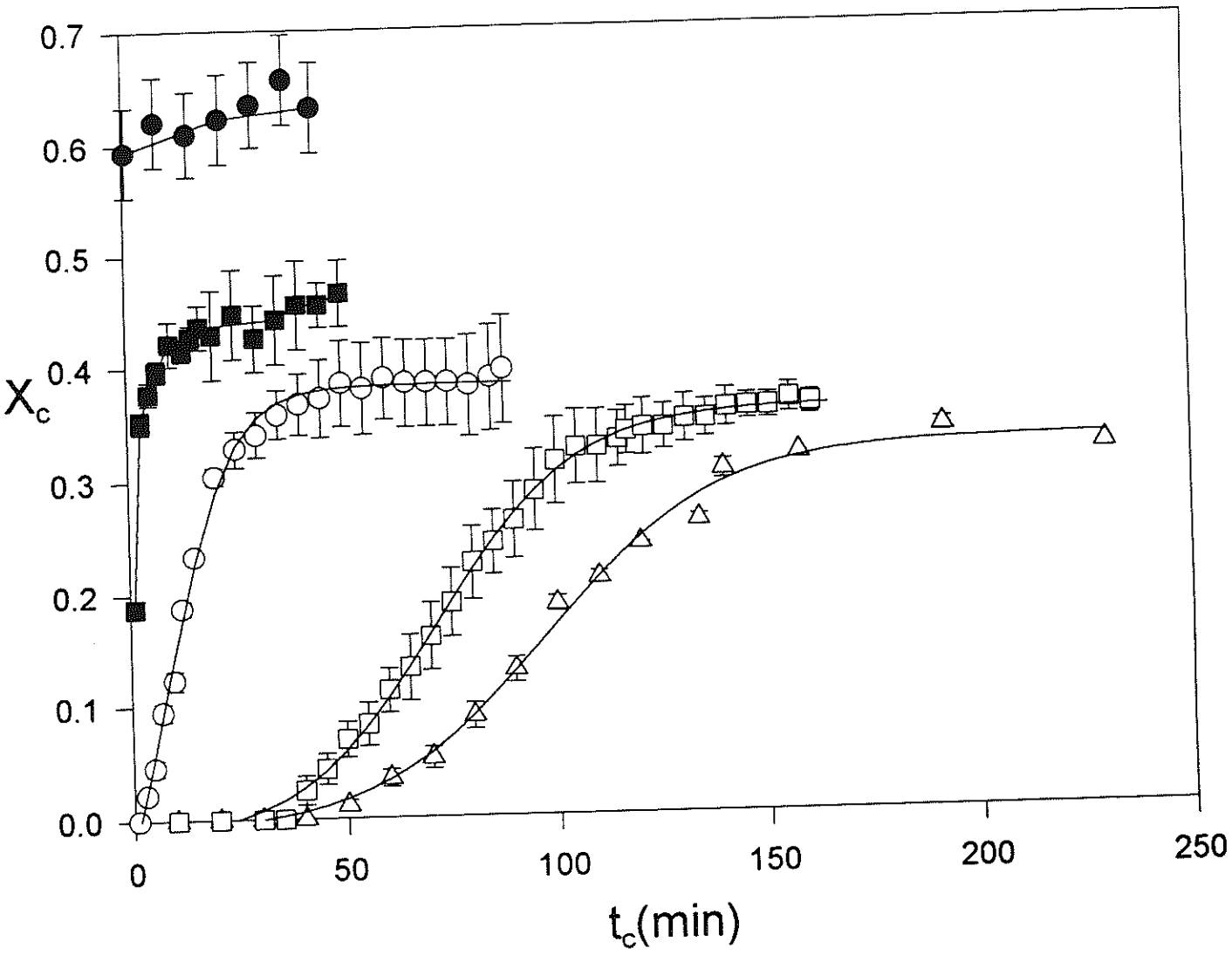

Fig.10

87:13

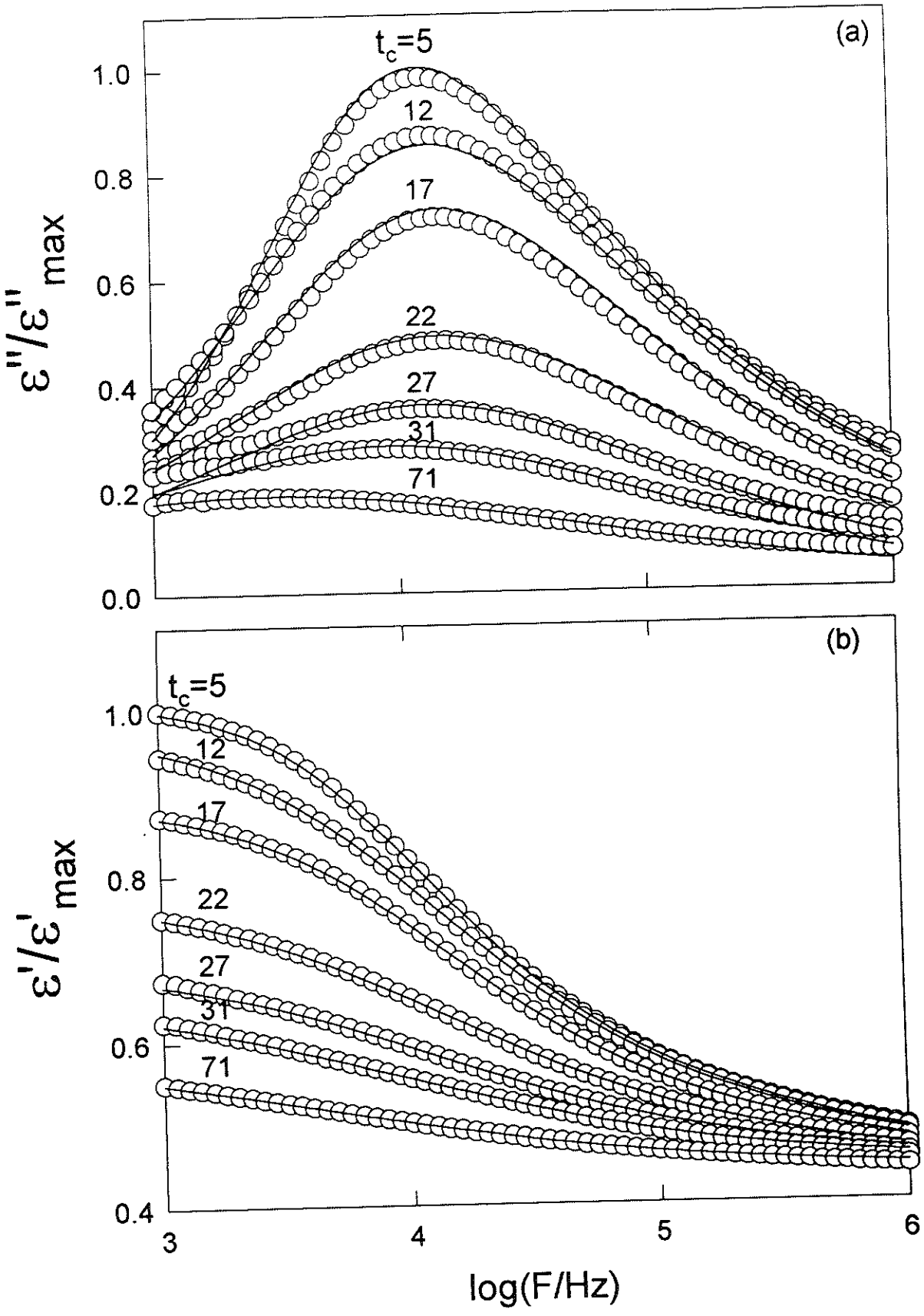
(a)
t_c=5
12
17
22
27
31
71
1.0
0.8
0.6
0.4
0.2
0.0
ε''/ε''max
(b)
t_c=5
12
17
22
27
31
71
1.0
0.8
0.6
0.4
ε'/ε'max
3
4
5
6
log(F/Hz)

Fig. 11

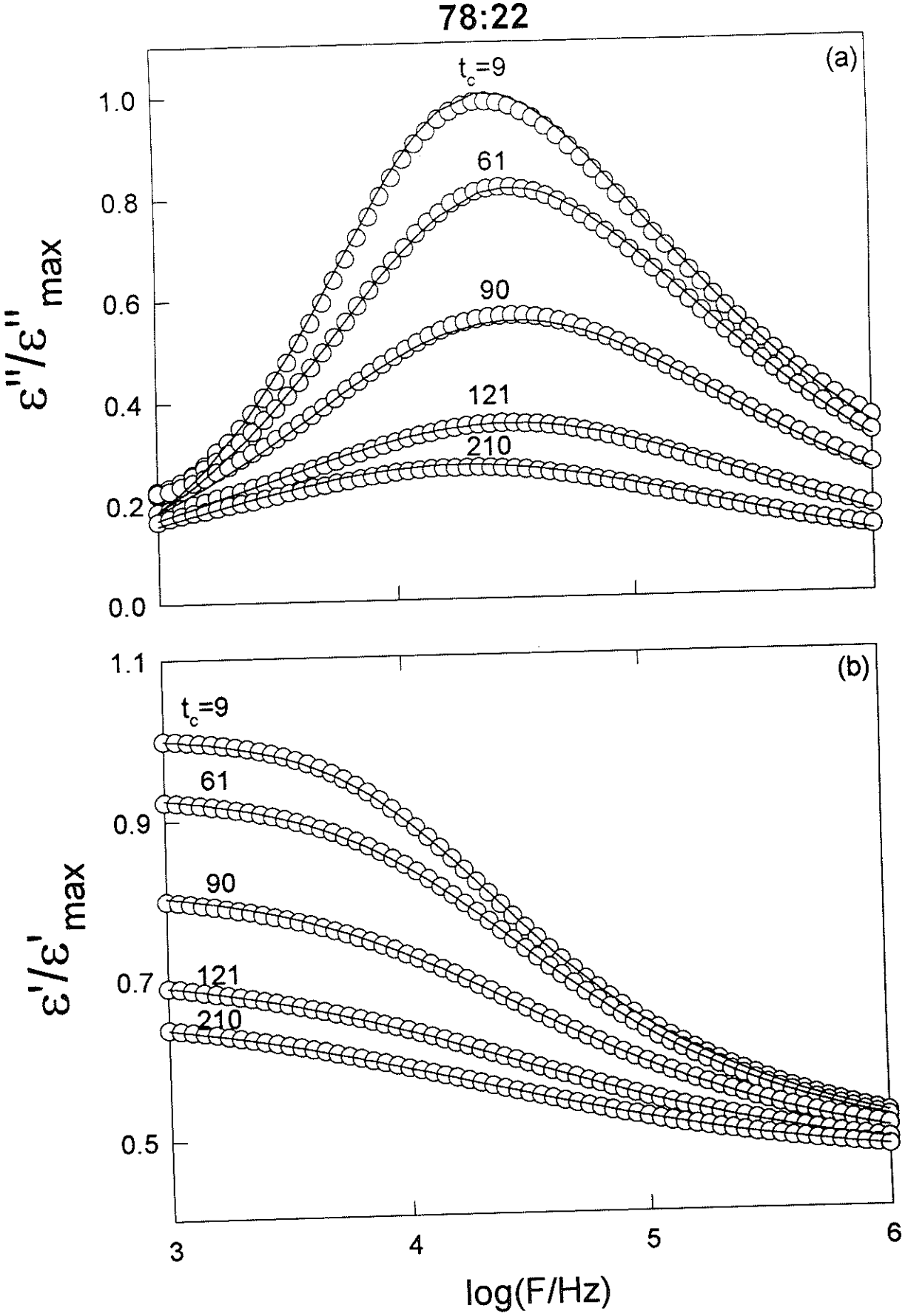
78:22
(a)
t_c=9
61
90
121
210
1.0
0.8
0.6
0.4
0.2
0.0
$\varepsilon''/\varepsilon''_{max}$
(b)
t_c=9
61
90
121
210
1.1
0.9
0.7
0.5
$\varepsilon'/\varepsilon'_{max}$
3
4
5
6
log(F/Hz)

Fig.12

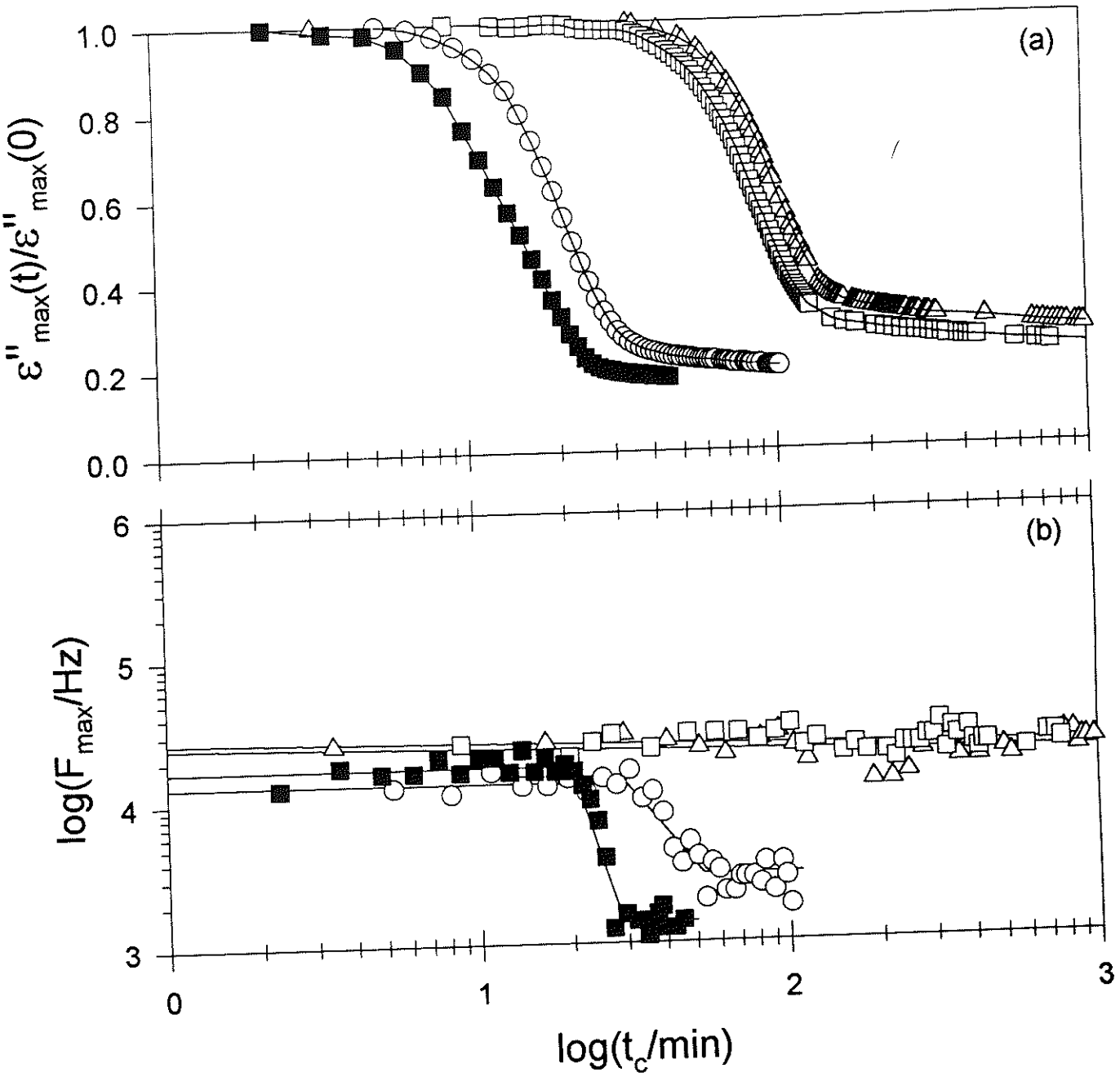

Fig. 13

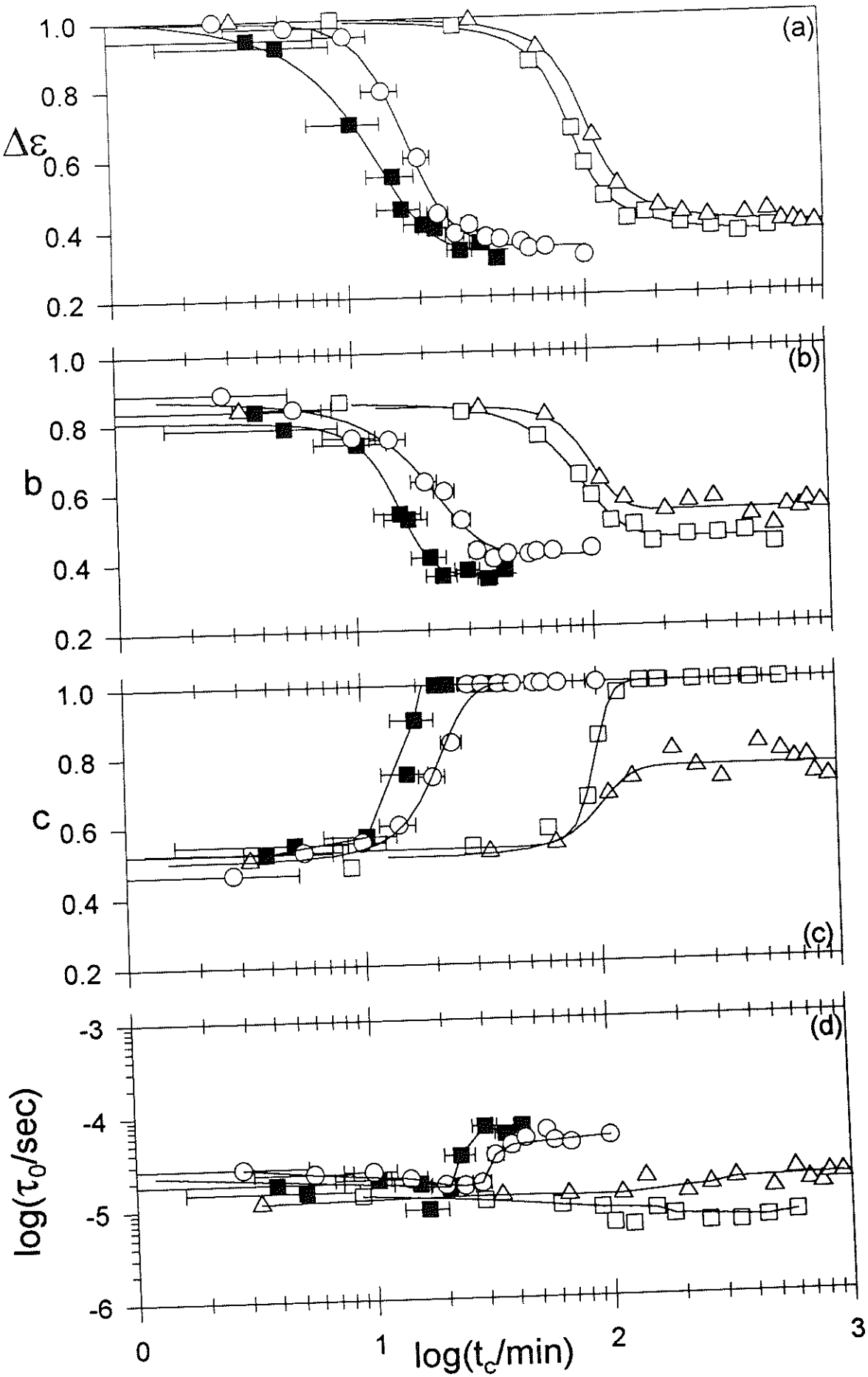
(a)
1.0
0.8
Δε
0.6
0.4
0.2
(b)
1.0
0.8
b
0.6
0.4
0.2
1.0
0.8
c
0.6
0.4
(c)
0.2
(d)
-3
-4
log(τ0/sec)
-5
-6
0
1
log(tc/min)
2
3

Fig. 14

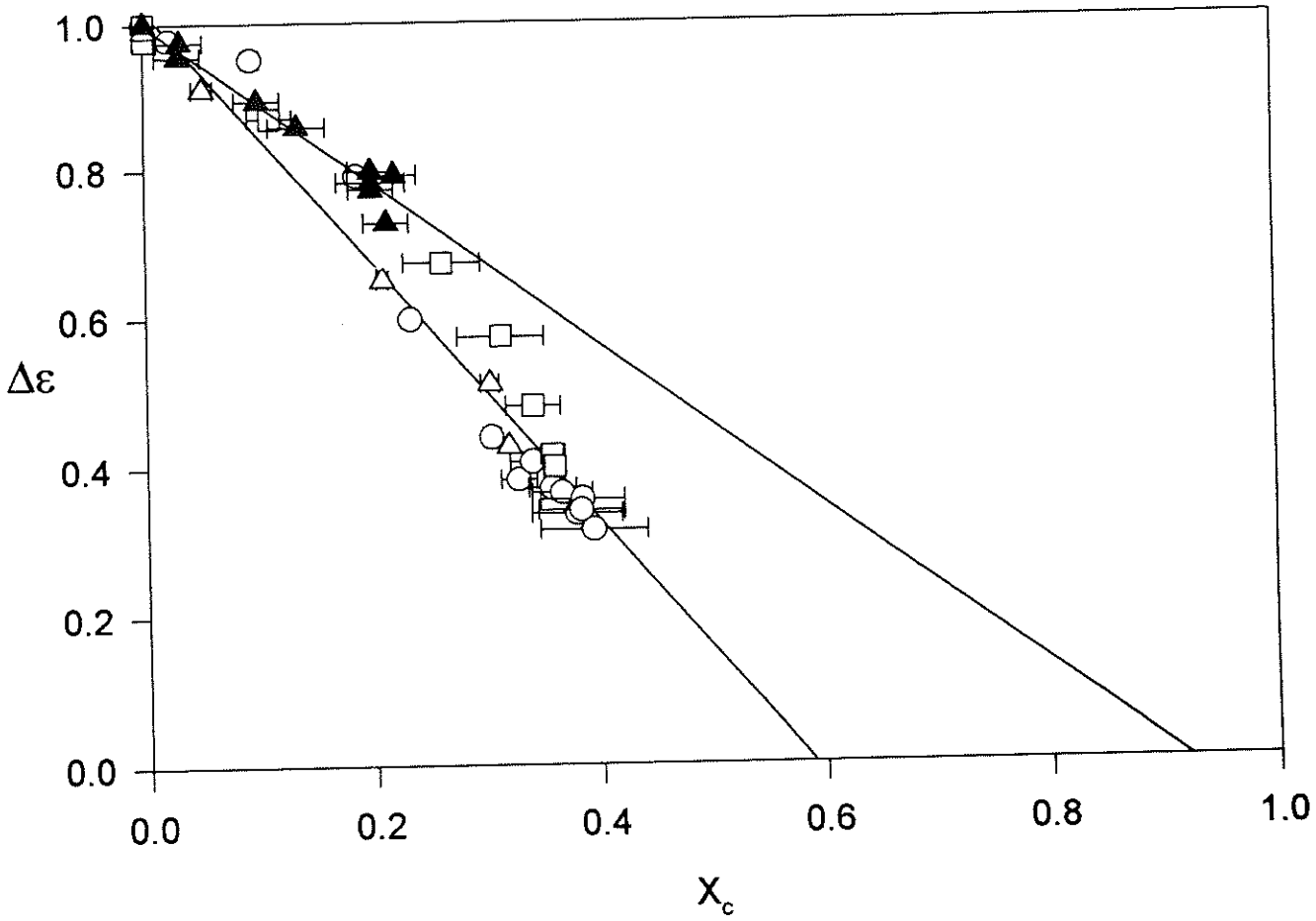

Fig. 15